Investigation of the stresses in rails

Secondary effects associated with the bending of a centrically loaded rail

PREFACE

Research on the stress distribution in a flexurally loaded rail was undertaken in connection with a graduation project, under the auspices of the Traffic Engineering and the Structural Mechanics Section, at the Delft University of technology. The investigations comprised strain gauge measurements and a computer analysis based on the finite element method.

Co-operation in a participatory or a monitoring capacity was given by:

Prof. Ir. B. van Bilderbeek
Prof. Ir. M. van Witsen
Ir. J. van 't Zand (Traffic Engineering Section)

Ir. A. W. M. Kok
Ir. C. F. Vrijman (Structural Mechanics Section)

Ir. F. P. M. Sopers (Applications and Systems Section, Computer Centre of the Delft University of Technology)

and the technical staff of the Laboratory for Highway and Railway Engineering, Delft University of Technology.

The object of the research was to test the existing theories describing this flexural behaviour and to obtain some idea of the degree of agreement between the two methods of investigation employed.

INVESTIGATION OF THE STRESSES IN RAILS
Secondary effects associated with the bending of a centrically loaded rail

Abstract

The flexural behaviour of a rail under purely vertical load acting in the plane of symmetry is investigated in this paper.

For this purpose a rail of NP 46 standard section was subjected to experimental research with the aid of electrical resistance strain gauges in the Laboratory for Highway and Railway Engineering (Stevin IV), Delft University of Technology. After some initial problems in maintaining the constancy of the conditions under which the measurements were performed, good results were obtained by this method.

Furthermore, the flexural stresses in the rail due to the above-mentioned load were analysed with the ICES/STRUDL application package, version 2, available at the University, by means of the IBM 360 computer of the University's Computer Centre. The two methods of determining the flexural stresses were found to be satisfactorily serviceable for the purpose and to yield comparable results.

It also emerged that the existing theories for calculating more particularly the maximum stresses occurring in the rail do not always yield satisfactory results. The system of mechanical relationships with which Prof. Dr. Ing. J. Eisenmann, Technological University of Munich, and other investigators describe the flexural behaviour of a rail under centric loading does not represent the actual behaviour of the rail under such loading. A better, qualitative, description of the flexural stress distribution in the rail cross-section under the applied load can be obtained by formulating the equilibrium conditions more satisfactorily and by introducing horizontal compatibility into the model.

Investigation of the stresses in rails

Secondary effects associated with the bending of a centrically loaded rail

1 Introduction

The rail performs a dual function in railway engineering. On the one hand, it is the supporting and load-distributing element of the permanent way; on the other, it is needed for vehicle guidance. The requirements imposed upon the rail by this dual function have led to the present cross-sectional shape: a relatively heavy upper part, the "head", a fairly narrow intermediate part, the "web", and a wide bottom flange, the "foot".

This shape has been found satisfactory in practice. Yet it has hitherto not been possible to obtain a detailed insight into the stress distribution in the rail cross-section when the rail is loaded in bending by the passage of a wheel or in general by a point load. The question is considered in this paper.

It has already long been known that the stress distribution in a rail loaded by a vertical force acting downwards at the axis of symmetry of the rail cross-section differs from the stress distribution that could be expected on the basis of prismatic beam theory, which assumes plane sections to remain plane. Besides a maximum tensile stress at the underside of the foot and a maximum compressive stress at the top of the head of the section, there also occur large tensile stresses directly below the head in consequence of the particular cross-sectional shape. Fig. 1 shows this shape and also indicates the stress distribution found to occur.

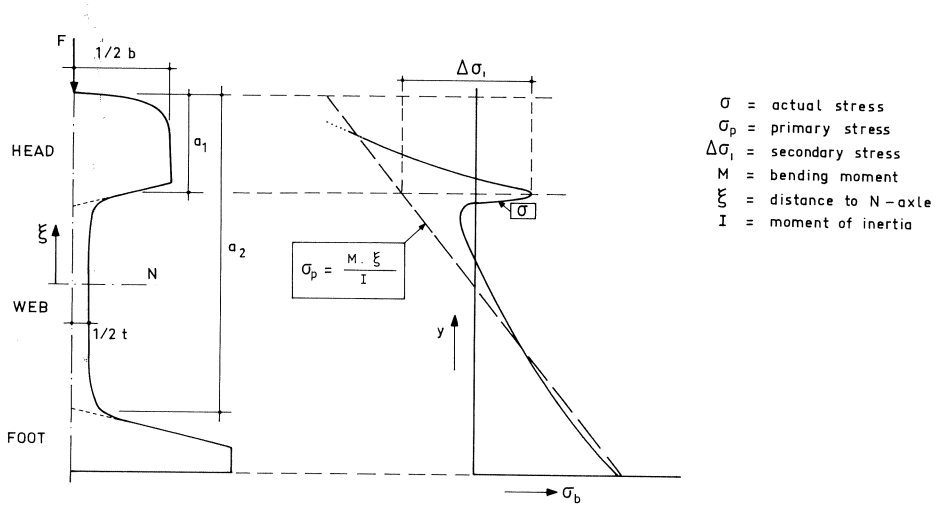

Fig. 1. Stresses as a result of a flexural moment in the cross-section in which the point of load-application occurs.

So far as the present authors are aware, the above-mentioned phenomenon was first investigated by Timoshenko and Langer [1], who explain it as follows: The rail as a whole behaves *primarily* as a flexural beam. As a result of this a linear stress distribution develops over the depth of the rail section, with pressure in the head and tension on the foot.

In addition, a *secondary* effect occurs. Since the web possesses relatively low stiffness with regard to vertical deformation, the head can behave in the manner of a beam elastically supported by the web. Under the influence of the vertical wheel load the head sinks (very locally) into the web, as it were. This results in extra compression at the top of the head and extra tension at the underside of the head. The overall stress configuration is obtained when the *primary* and the *secondary* flexural behaviour are superimposed upon each other.

Timoshenko and Langer have attempted to establish an analysis for this behaviour. They conceive the primary and the secondary flexural behaviour as two mutually independent phenomena, so that the resultant stress distributions are superimposable. The stress distribution due to the primary flexural behaviour is analysed in accordance with conventional prismatic beam theory:

$$\sigma = M \cdot \xi / I$$

where:

σ = flexural stress in N/mm^2
M = bending moment in Nmm
ξ = distance from point under consideration to neutral axis in mm
I = moment of inertia in mm^4

The secondary flexural behaviour is analysed with the theory of Winkler and Zimmermann for elastically supported prismatic beams [2]. In this approach a cut is assumed to be applied between the head and the web. Other basic assumptions of this theory are:
- linear-elastic material behaviour;
- plane sections remain plane (Bernoulli's hypothesis);
- the deflections are very small in relation to the length of beam under consideration;
- the base (supporting medium) is schematized as an assembly of linear-elastic springs;
- there are no shear stresses at the beam/base interface and in the base.

With these initial assumptions and adopting a stiffness against vertical deformation of the base defined as follows:

$$k = \frac{\text{modulus of elasticity} \times \text{web thickness}}{\text{web depth}}$$

Timoshenko and Langer arrive at a formula for determining the secondary stress:

$$\Delta\sigma = 1{,}5F \sqrt[4]{\frac{a_3}{3b^3 a_1^5 d}}$$

where:

$\Delta\sigma$ = secondary or additional stress (N/m^2)
F = force constituting the load (N)
a_1 = depth of the head (m)
a_3 = depth of the web (m)
b = width of the head (m)
d = thickness of the web (m)

In 1965, Eisenmann of the Technological University of Munich published an article on the same subject [3]. He also tries to develop an analysis for the stress distribution. His approach is similar to that of Timoshenko and Langer, except that the stiffness of the web against vertical deformation is determined in a different way. For this purpose Eisenmann uses the theory for a plate bounded on one side [3]. The resulting formula is as follows:

$$\Delta\sigma = 1{,}5F\sqrt[4]{\frac{\ln\,(a_2/a_1)}{3b^3a_1^4d}}$$

where:

$\Delta\sigma$ = secondary or additional stress (N/m^2)
F = force constituting the load (N)
a_1 = depth of the head (m) (see also Fig. 2)
a_2 = distance between top of head and top of foot (m)
b = width of the head (m)
d = thickness of the web (m)

The head of the rail section is schematized to a rectangle with dimensions a_1 and b as indicated in Fig. 2. Just how these dimensions should be chosen is not explained. From the table accompanying Fig. 2 it emerges that more particularly the magnitude of a_1 has a considerable effect on the magnitude of the calculated additional stress.

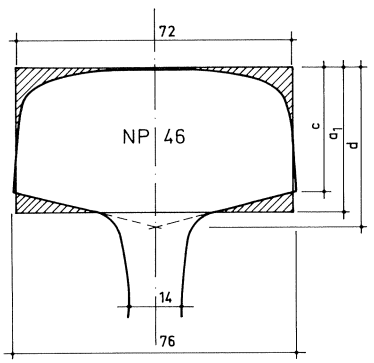

Fig. 2.
The fixation of the average depth of the head (a_1).

Table 1.
Illustration of the impact of the value of a_1 (i.e. the average depth of the head) on the value of the secondary stress, when calculated with the aid of Eisenmann's formula:

$$\Delta\sigma_1 = \frac{3}{2}F\sqrt[4]{\frac{\ln\,a_2/a_1}{3b^3a_1^4d}}$$

in which: $a_2 = 117$ mm, $b = 74$ mm, $d = 14$ mm, $F = 100$ kN

a_1 (mm)	secondary stress (N/mm^2)
33.0	75.1
35.0	69.9
37.75	63.8
40.0	59.4
42.5	55.1

Eisenmann's formula is found sometimes to give too high values (up to 10% too high) in practice. This is not very surprising when it is considered that Eisenmann, like Timoshenko and Langer, neglects the horizontal compatibility between the head and the web and thus schematizes the rail to a more flexible structure than it actually is. Besides, as has emerged from the research reported below, Eisenmann's theory does not satisfy the conditions of equilibrium.

2 Research

2.1 *Laboratory work*

The research, which was undertaken within the context of a graduation project, was of limited scope. It was carried out in the Laboratory for Highway and Railway Engineering (Stevin IV) of the Department of Civil Engineering in the Delft University of Technology. Although the type of rail section (more particularly the moment of inertia and/or the section modulus, and the dimensions a_1, a_2 and b in Eisenmann's formula) is an important variable in the problem under investigation, only the NP 46 standard rail section extensively used in the Netherlands was investigated.

The research work involved a so-called three-point bending test. The bearings chosen for the purpose were triangular in section, rounded at the apex, which supported the rail across the full width of the foot ("gable roof shape"). The loading was applied with the aid of a hydraulic jack and transmitted through a contact piece likewise of triangular shape, i.e., similar to the bearings, but with the rounded apex downwards. In this way a

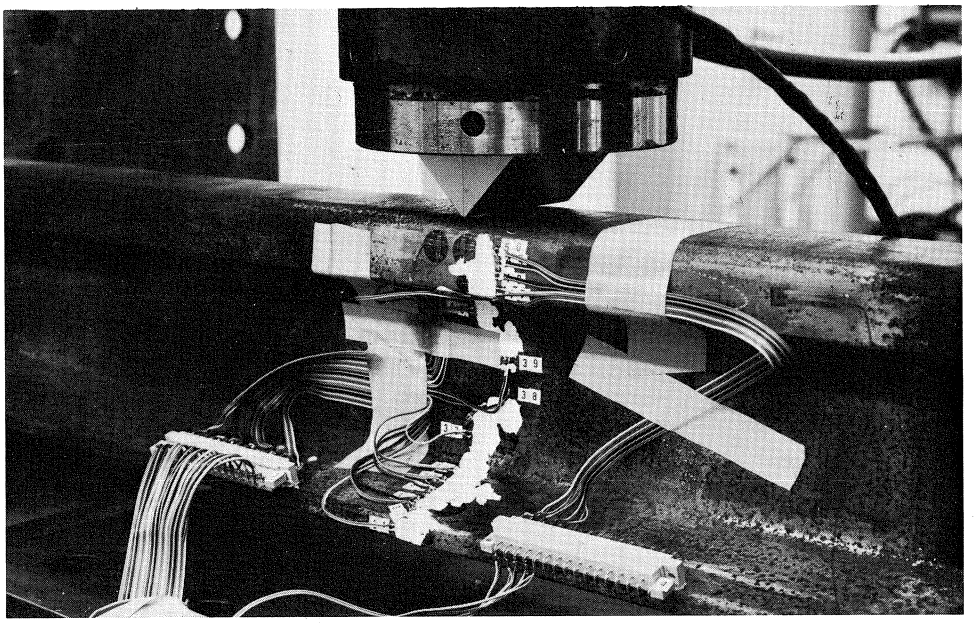

Fig. 3. Cross-section with strain gauges.

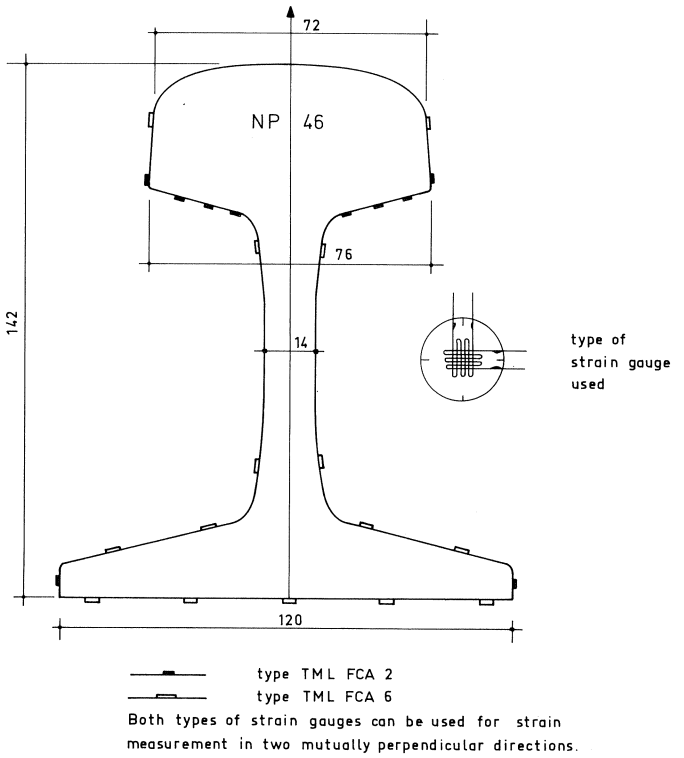

Fig. 4. The positions of the strain gauges.

narrow elongated contact face perpendicular to the longitudinal direction of the rail was obtained (see Fig. 3).

The force acting on the specimen was always directed vertically downwards and could be steplessly varied. The loads applied in practice were 40, 60, 80 and 100 kN. Later on, only 60 and 100 kN were applied.

The measurements were performed with two types of electrical resistance strain gauges, both comprising two mutually perpendicular windings of constantan wire in a flat supporting material. In this way it was possible to measure the strains in two mutually perpendicular directions (see also Fig. 4). At those points where large stress gradients were to be expected, strain gauges with 2 mm gauge length were affixed. Elsewhere, gauges having a gauge length of 6 mm were considered adequate for the purpose. 25 strain gauges were affixed along one cross-section. The positions of the gauges is shown in Fig. 4.

For practical reasons the measurements were performed on a piece of NP 46 rail with a length of 1 m, while three different span lengths (distances between bearings) were employed, namely, 500, 700 and 900 mm. As the rail was able to slide in the axial direction on the bearings, the same strain gauges could be used for carrying out measurements at varying distances from the load. This was possible because the dead weight of the rail was negligible in relation to the applied load.

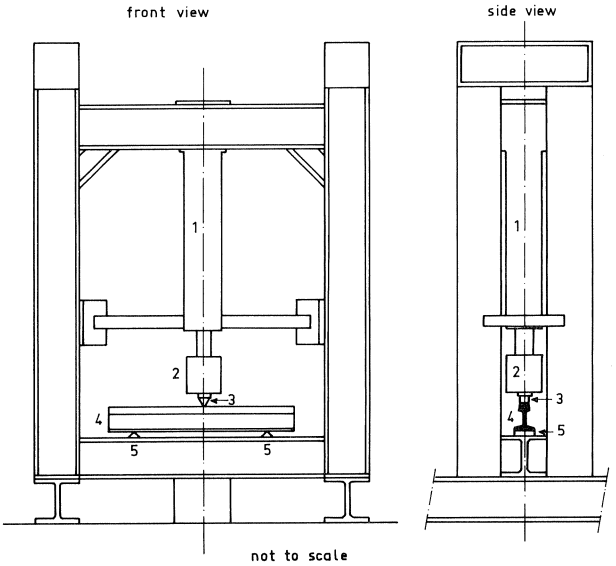

Fig. 5. The test arrangement.

explanation
1. Hydraulic jack
2. Pressure gauge
3. Contact piece
4. The tested piece of rail (type NP 46)
5. Supports

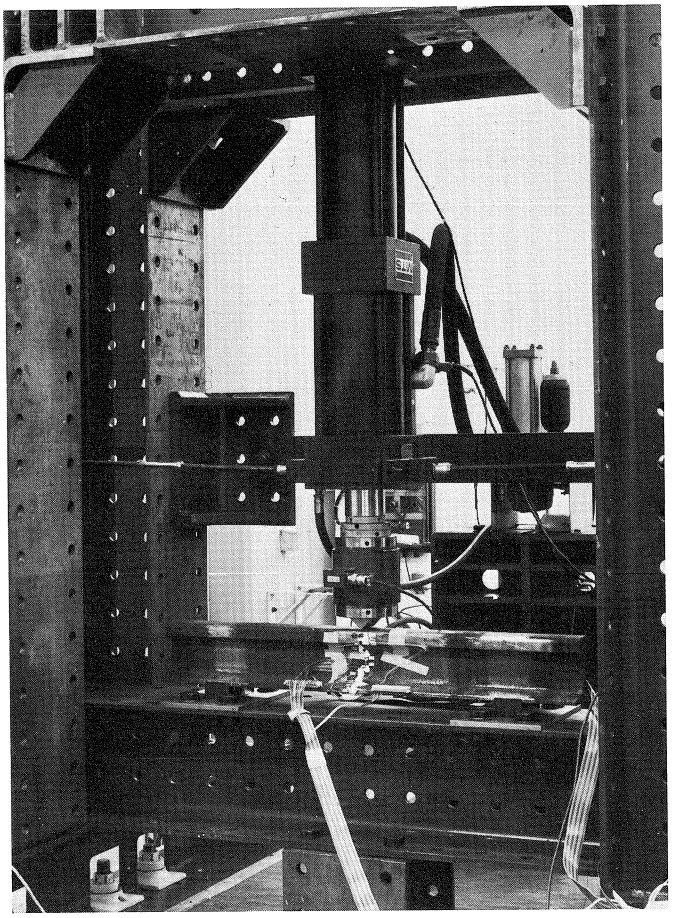

Fig. 6. View on the test arrangement.

The rail specimen and the hydraulic jack were mounted in a frame constructed of heavy I-section members on a practically vibration-free foundation. This arrangement is shown in Figs. 5 and 6.

In the strain gauge measurements the most commonly employed technique was adopted, namely, the *carrier wave system.* For this purpose the so-called *"half bridge circuit"* was used, which is compensated for temperature influences (see Figs. 7 and 8). As only one strain gauge at a time could provide a reading on the meter, it was necessary alternately to energize one of the gauge windings by means of a selector switch. Switch boxes developed by the Laboratory for Highway and Railway Engineering were used for this purpose. Further information is given in [4].

The actual measuring program had to give a clear insight into the stress pattern. The stress distribution both along the edge of the rail section at one cross-section and in the axial direction is important in connection with this. Also, the effect of the magnitude of

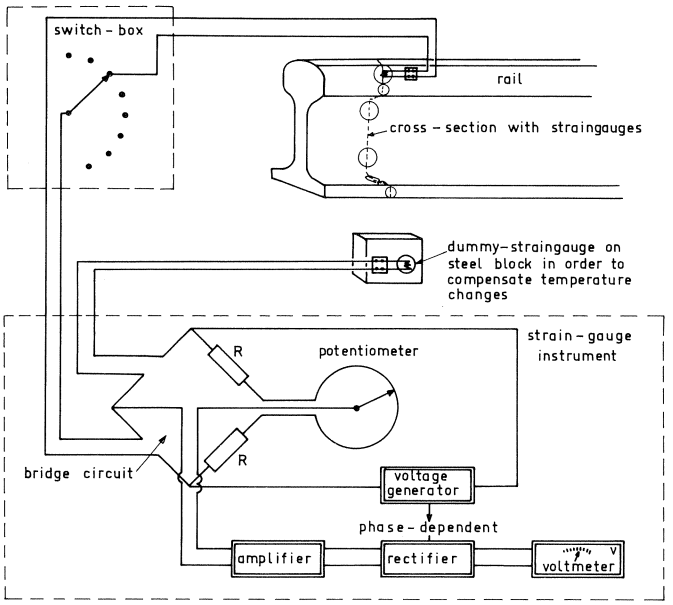

Fig. 7. The electric circuit in principle.

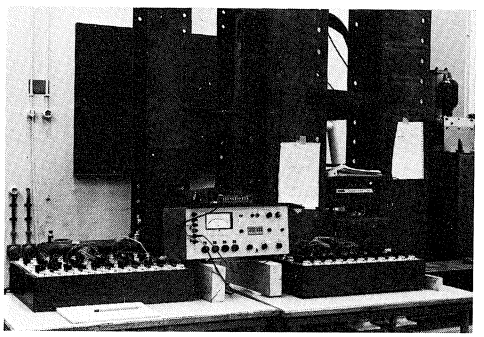

Fig. 8. View on the electric arrangement; the strain-gauge instrument and the switch-boxes.

the load and of the span had to be investigated, and these two last-mentioned quantities – load and span – were adopted as variables.

Measurements were performed with varying positions of the measuring cross-section in relation to the mid-span point. In this way a large number of measured data was obtained, which were processed with the aid of ALGOL computer programs to yield utilizable representations of the stress distribution.

2.2 *Computer analysis*

A rail of NP 46 standard section was numerically analysed for the case of the same three-point bending test as that in the laboratory arrangement, but only for a load of 100 kN and a span of 700 mm. The calculations were performed with the aid of the ICES/STRUDL (Integrated Civil Engineering System/Structural Design Language) program package which is available at the Computer Centre of the Delft University of Technology and which is based on the *finite element method* [5]. In this method the structure under consideration is split up into a number of parts, the so-called finite elements. The elements adopted for the rail cross-section and for the longitudinal direction are shown in Figs. 9 and 10.

In the computer analysis a set of equations has to be solved. Because of the complicated geometric structure of the rail section and the large number of elements, the number of equations is considerable, requiring a great deal of computer time. In order to

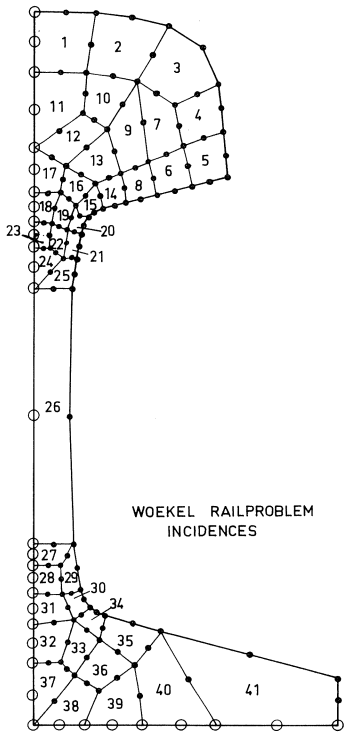

Fig. 9. The position of the elements in the cross-section.

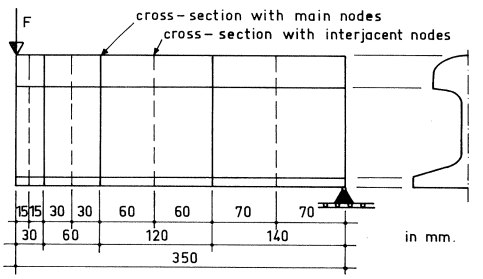

Fig. 10. The position of the elements in longitudinal direction.

keep the whole computing process properly under control, the program has been so adapted that the set of equations can be solved in steps. If the computer time reserved by the user has been used up before the analysis has been completed, the program can be stopped and the intermediate results stored. These data are re-introduced in the next run, enabling the analysis to be continued. For a review of the computer work see [4].

3 Results

The results obtained in the laboratory measurements and those analytically obtained with the computer are shown, for the loading case with $F = 100$ kN and a span of 700 mm, in Fig. 11. There is good agreement between the two sets of results.
Since the maximum value found for the additional stress $\Delta\sigma_1$ in the measurements and in the analysis was 63 N/mm^2, it can be concluded that, if it is desired to retain the schematization of the rail head as a rectangle, it is necessary to adopt for a_1 a value which is approximately the arithmetical mean of c and d (see Fig. 2). With this value of a_1 good results are obtained with Eisenmann's formula, for the NP 46 rail section anyway.

The phenomenon of secondary bending is very local in character. At a distance of about 60 mm in the axial direction from the point of load application an approximately linear stress ditribution is already found (see Fig. 12).

As appears from Fig. 13, the total flexural stress at the underside of the head corresponds to a curve oscillating about the primary stress with increasing distance from the load application point, but not in accordance with the theory of elastically supported

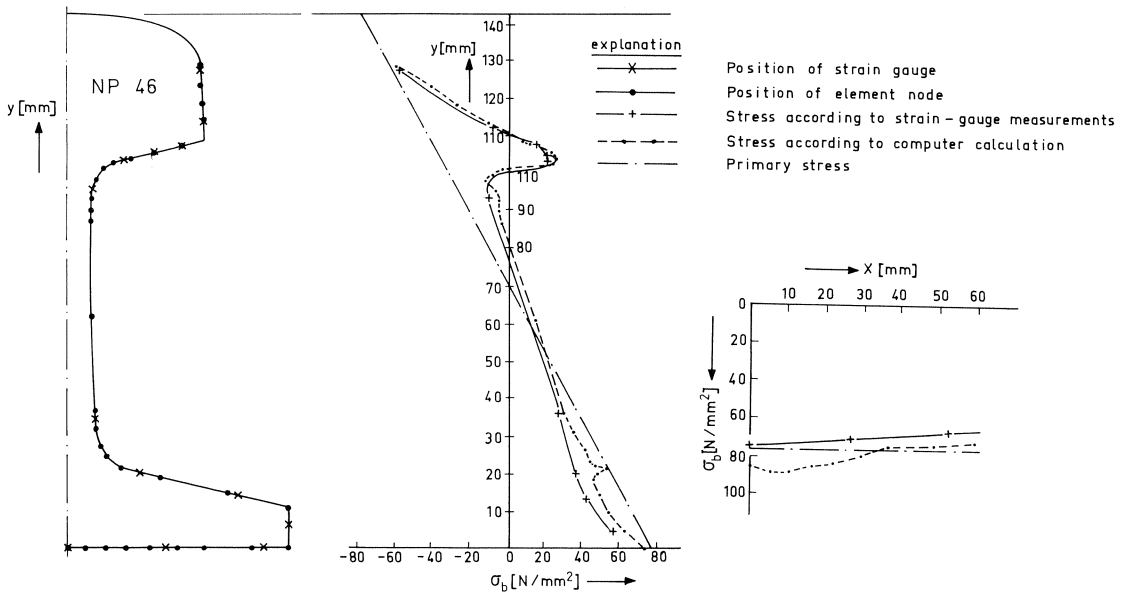

Fig. 11. Flexural stresses σ_b in the cross-section in which the point of load-application occurs. Load F is 100 kN. Distance between the supports is 700 mm.

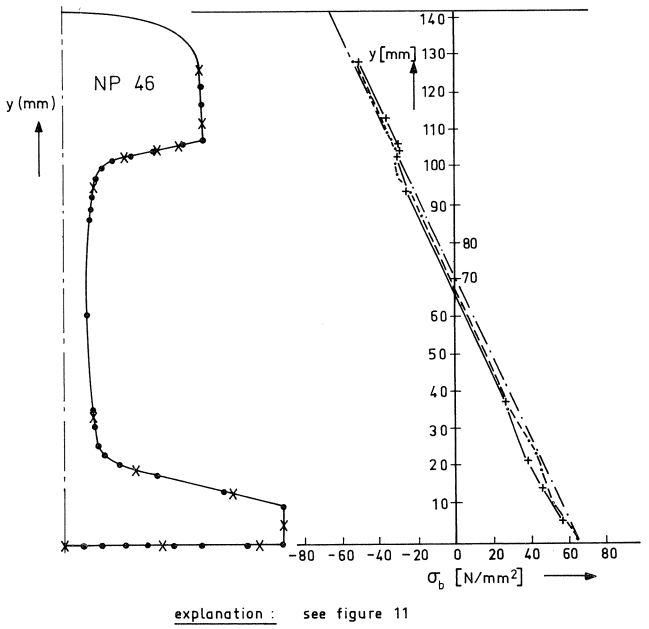

Fig. 12. Flexural stresses σ_b in a cross-section at a distance of 60 mm from the point of load-application. Load F is 100 kN. Distance between the supports is 700 mm.

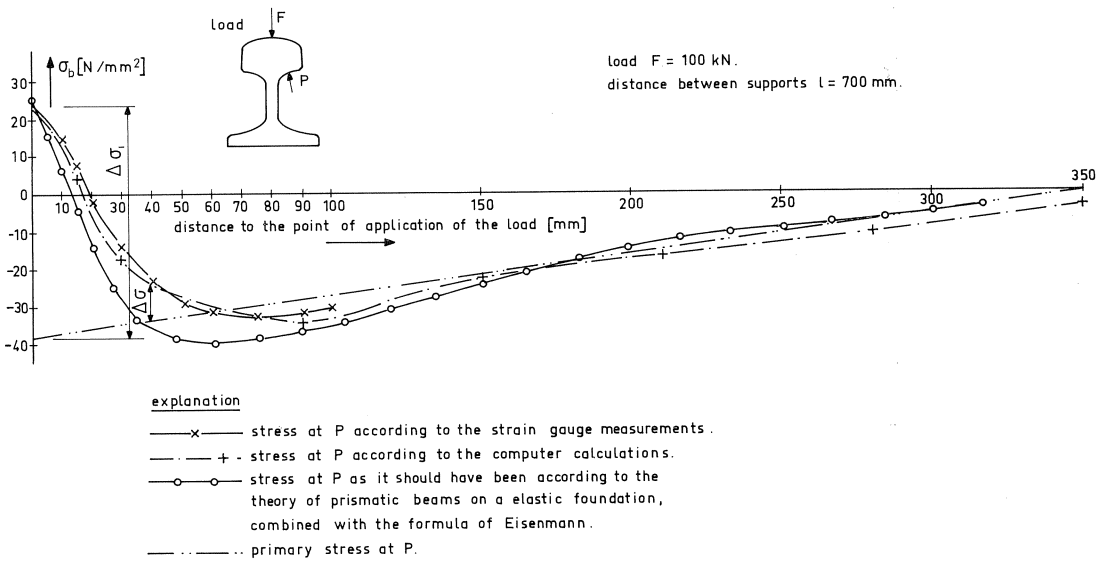

Fig. 13. Total stress as a function of the distance to the point of application of the force at a position P at the underside of the rail-head (Y-coordinate = 105,4 mm).

beams as supposed by Eisenmann. The stress distribution conforming to this latter theory is also shown for comparison.

The magnitude of the flexural stresses in the longitudinal direction is, for each point of the rail cross-section, directly proportional to the magnitude of the load. The magnitude of the additional stress $\Delta\sigma_1$ is found to be independent of the span (distance between bearings).

The flexural tensile stress along the lower edge of the rail foot attains its maximum value at the centre-line of the rail and decreases by about 15% across the width of the foot towards the edges (see Fig. 11). The maximum can be calculated with the aid of the primary theory.

If the strain gauges were affixed at a distance of, say, 1 cm from the centre of the rail foot – as might occur in measurements performed in situ on the track, under conditions in which it is not possible to achieve great accuracy – the resulting maximum error in the stress measurement would be under 3%. This means that, when such a relation between a stress determined with the aid of a strain gauge and the horizontal force is known, a rail can in principle be utilized as a measuring transducer. In that case, taking account of the subgrade and the type of fastenings, it is possible to calculate from the strain gauge readings what magnitude the actual wheel load must have had.

Eisenmann has attempted to resolve the actual stress distribution, indicated schematically in Fig. 14, into a "primary stress distribution" (a) and a "secondary stress distribution" (b) in the head. He determines the magnitude of the "secondary stress" with the theory of the elastically supported beam, the web of the rail being conceived as the elastic support. The "primary" and the "secondary stress distribution" together, however, do *not* constitute a system in equilibrium with the external loading, inasmuch as the "primary stress distribution" produces a "primary moment"which by definition is in equilibrium with the external loading. The "secondary stress distribution" produces a "secondary moment" which is not compensated in Eisenmann's schematization. Hence a "tertiary moment" will be needed in order to equilibrate the "secondary moment".

This "tertiary moment" will in turn produce a "tertiary stress distribution" in the rail section, with tension at the top and compression at the bottom. From the calculations and measurements it emerges that this is indeed the case (see also line c in Fig. 14).

If it is desired to calculate the magnitude of the tertiary stresses, two approaches are

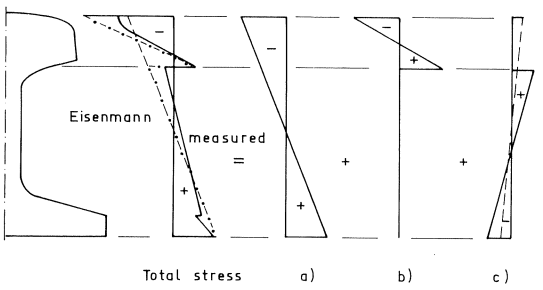

Fig. 14. Stress distribution in diagram.

obvious. The tertiary moment can be conceived as being resisted by the whole rail section or, alternatively, by only the web and foot acting as a kind of inverted T-beam, i.e., making use of the imaginary cut also adopted by Timoshenko and Langer and by Eisenmann. From the overal stress distribution determined from the measurements and from the computer analysis it appears that a better approximation is found to lie in between these two alternative conceptions.

Eisenmann only calculates the additional stress at the head-to-web junction, but the calculated secondary moment of course acts on the entire head of the rail. As appears from Fig. 14, the line corresponding to Eisenmann's theory certainly does not describe the actual behaviour of the rail in bending; the neutral axis for the secondary bending of the head is in reality located higher than would be expected on the basis of the theory (i.e., at mid-depth of the reactangular schematization of the head).

We offer the following explanation to account for this:

As Fig. 15 shows, according to Eisenmann's model, a discontinuity in the stress distribution occurs at the head-to-web junction. This discontinuity is somewhat reduced as a result of the introduction of the above-mentioned tertiary moment. Such a stress discontinuity cannot, however, actually occur in a homogeneously elastic material. The stresses at the "interface" must, as it were, be drawn together. This affects the stress distribution both in the head and in the web, with diminishing effect according as the distance to the interface is larger. It is reasonable to suppose that at the top of the head the effect of this phenomenon will have diminished so as to be hardly noticeable. Thus, at the top of the head there is no change in stress distribution as compared with Eisenmann's conception (with or without the tertiary moment), but nearer the interface at the junction of head and web the difference in stress distribution will become greater. The stress distribution indicated in the right-hand diagram of Fig. 15 is due to this.

From Fig. 16 it appears that the flexural behaviour in accordance with Eisenmann's theory, as so far described, does indeed occur, subject to some adjustments for the points located along the edge of the rail section. This is not the case in the "interior" of the section, however. At the axis of symmetry of the section a significantly different stress distribution occurs, as the computer analysis indicates. For the web and foot the differences are not very considerable, but they are very marked in the head. Because of the fact that at the symmetry axis of the rail section the underside of the head is supported by the web, the secondary deflection of the head at this axis is smaller than the secondary deflection of those parts of the head which are not directly supported by the web. This explains why the secondary stress at the bottom of the head is greater along the edge than at the axis of symmetry of the rail section.

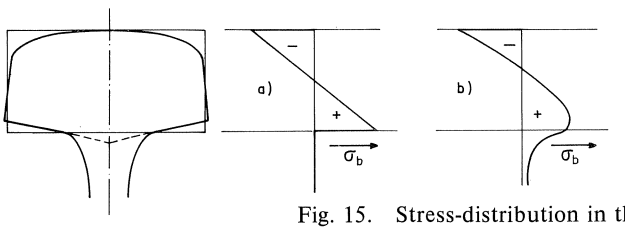

Stress distribution in the head as a result of the secondary moment
a) according to Eisenmann's formula
b) when horizontal compatibility is taken into account as well.

Fig. 15. Stress-distribution in the head.

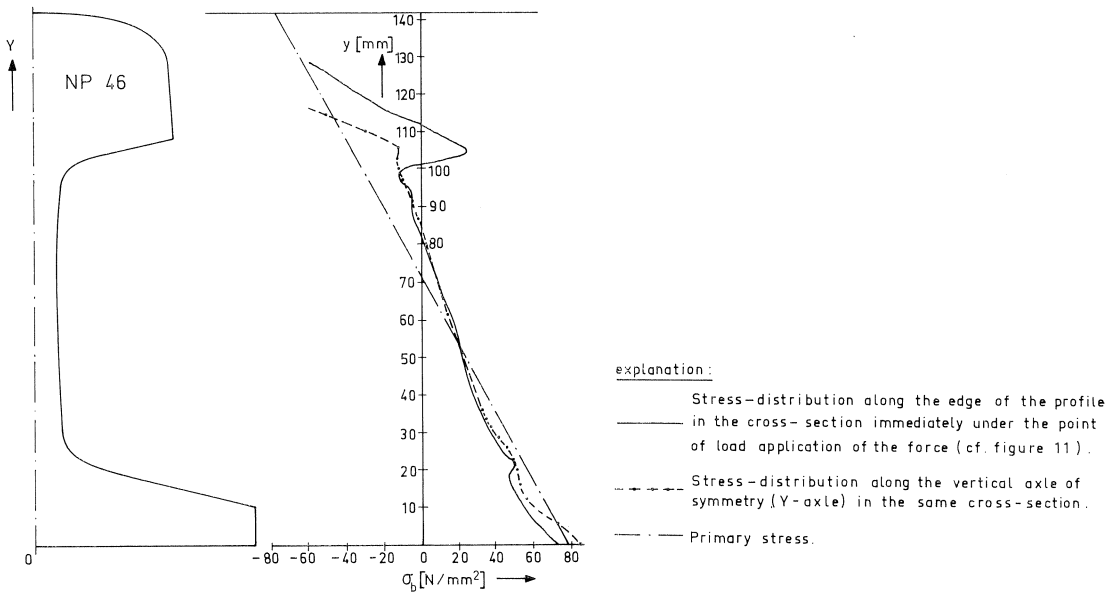

Fig. 16. Stress-distribution according to the computer calculations.

4 Conclusions

The secondary flexural stress can be calculated with reasonable accuracy by means of Eisenmann's formula, but the latter certainly does not adequately describe the flexural behaviour of a centrally loaded rail. A quantitative description of this complex behaviour in all its aspects will require further research. From the investigations reported here it emerges that both the computer analysis and the measurements obtained with electrical resistance strain gauges are suitably serviceable methods for the purpose.

References

1. Timoshenko, S. and B. F. Langer, Stresses in railroad track. American Society of mechanical Engineers ASME, 1931.
2. Zimmerman, H., Die Berechnung des Eisenbahnoberbaues (Railway permanent way design), 3rd ed., Ernst & Sohn, Berlin, 1941.
3. Eisenmann, J., Theoretische Betrachtungen über die Beanspruchung des Schienenkopfes am Lastangriffspunkt (Theoretical considerations on the stress conditions in the rail head at the point of load application), Eisenbahntechnische Rundschau ETR 14 (1965). No. 1/2, pp. 25-34.
4. Kolvoort, A. J. and T. Woestenburg, Sekundaire effekten bij buiging van een NP 46 spoorstaaf bij centrische belasting (Secondary effects in the bending of an NP 46 rail under centric loading), Graduation Project Report, Delft University of Technology, Department of Civil Engineering, Traffic Engineering Construction, Delft, September 1979.
5. Blaauwendraad, J. and A. W. M. Kok, Elementenmethode voor konstrukteurs, I en II (Finite element method for designers, I and II), Agon-Elsevier, Amsterdam, 1973.